Contribution from the Chemistry Department,
Marquette University, Milwaukee, Wisconsin 53233

# Electrochemical and Spectroscopic Studies of Iron Porphyrin Nitrosyls and Their Reduction Products

In-Kyu Choi, Yanming Liu, DiWei Feng, Ki-Jung Paeng, and Michael D. Ryan*

*Received May 5, 1989*

Fe(P)(NO), where P = TPP, TPC, or OEP, is reduced in three one-electron steps in nonaqueous solvents. The products of the first two waves ($Fe(P)(NO)^-$ and $Fe(P)(NO)^{2-}$) were stable, and the visible spectra were obtained by using OTTLE spectroelectrochemistry. The vibrational spectra of Fe(P)(NO) and its first reduction product obtained coulometrically were recorded. The porphyrin vibrations for both species were consistent with low-spin ferrous complexes. The $\nu_{NO}$ and $\nu_{Fe-N}$ bands could also be observed for both complexes, though $\nu_{NO}$ for $Fe(TPP)(NO)^-$ was quite weak. For Fe(TPP)(NO), $\nu_{NO}$ ($^{15}N$ values in parentheses) was 1681 $cm^{-1}$ (1647 $cm^{-1}$) and $\nu_{Fe-N}$ was 525 $cm^{-1}$ (517 $cm^{-1}$). Upon reduction, $\nu_{NO}$ decreased to 1496 $cm^{-1}$ (1475 $cm^{-1}$) while $\nu_{Fe-N}$ increased to 549 $cm^{-1}$ (538 $cm^{-1}$). These results were consistent with the addition of the electron to the half-filled $d_{z^2} + \sigma_N$ orbital, which is formed from $\pi^*_{NO}$ and iron $d_{z^2}$ orbitals. Therefore, addition of an electron to this orbital would lead to a strengthening of the Fe–N bond and a weakening of the N–O bond. Dc polarography of Fe(TPP)(NO) and Fe(TPC)(NO) was carried out in the presence of several substituted phenols. The limiting current and half-wave potential of the first wave were unaffected by the presence of the phenols, except at high phenol concentrations. A new second wave appeared, though, in the presence of phenols, and the limiting current and half-wave potential for this wave depended strongly on the concentration and identity of the weak acid. The overall reduction appeared to involve three electrons on the polarographic time scale, to yield $Fe(P)^-$ and hydroxylamine. Further reduction to ammonia was observed on the coulometric time scale. Exhaustive electrolysis gave ammonia in nearly quantitative yield for 2-chlorophenol concentrations greater than 20 mM. No differences were observed in the polarographic behavior of Fe(TPP)(NO) and Fe(TPC)(NO), but somewhat higher concentrations of 2-chlorophenol were needed to generate ammonia coulometrically.

## Introduction

The enzymatic reduction of nitrate to ammonia is catalyzed by a class of enzymes called the assimilatory nitrite reductases. These enzymes, commonly found in plants, contain siroheme and a 4Fe-4S cluster in their native form.[1] Sulfite reductases, which are also able to carry out the reduction of nitrite to ammonia, are large, complex enzymes, but they can be dissociated into a functioning subunit that has a single siroheme and a 4Fe-4S cluster.[2] The catalytic reduction of nitrite proceeds via the formation of a siroheme–nitrosyl complex, which is then reduced to ammonia.[2-4] The nitrosyl complex has been observed experimentally and is the major species present during turnover.[4] While no other intermediates have been observed in the operating enzyme, hydroxylamine can be reduced by the enzyme, though at a slower rate than nitrite, and is thought to be an intermediate in the reduction. The details of the reduction are not known, and it has been the aim of several research groups to characterize intermediates in the reduction and to elucidate the reduction mechanism using model porphyrin complexes.[5-11]

Previous work has shown that iron porphyrin nitrosyls are reduced in two one-electron steps in nonaqueous solvents.[7,8] The visible spectra of Fe(P)(NO) (where P = TPP, OEP, OEC, and OEiBC[9]), and their reduction and oxidation products, were obtained by using thin-layer spectroelectrochemistry[7] or coulometry.[8] The reduction product, $Fe(P)(NO)^-$, was stable in butyronitrile but was reoxidized in methylene chloride.[7b] The effect of axial coordination by pyridines on the half-wave potentials of Fe(P)(NO) complexes was recently examined.[12] Pyridine and substituted pyridines coordinate weakly with Fe(P)(NO) but dissociate when the complex is reduced.

The electrochemistry of a water-soluble iron porphyrin, Fe(TPPS) (TPPS = dianion of tetrakis(4-sulfonatophenyl)porphyrin), in the presence of nitrite was examined in detail by Meyer et al.[10,11] Under the pH conditions used, nitrite disproportionated to form $[Fe^{II}(NO^+)(TPPS)]^{3-}$, which was reduced readily to $[Fe^{II}(NO^\cdot)(TPPS)]^{4-}$. Further reduction of this complex to $Fe^{II}(NO^-)$ occurred at −0.64 V vs SCE, which was independent of pH for pH values greater than 2.6. At pH values less than 2.6, protonated complexes, $Fe(NHO)(TPPS)^{4-}$ and $Fe(NH_2O^+)(TPPS)^{3-}$, were postulated. Protonation of $NO^-$ and dimerization led to $N_2O$, while further reduction (with protonation) led to hydroxylamine and ammonia. The yields of nitrous oxide, ammonia, and hydroxylamine were determined from controlled-potential electrolysis under catalytic conditions.

While the electrochemistry of the nitrosyl complexes, as well as the overall products of the electrolysis, has been examined, the details of the reduction mechanism are still not clear. In this report, we will characterize the structure of the one-electron-reduction product using visible and resonance Raman spectroscopy. Once this product has been characterized, the reaction of the one-electron-reduced product with strong bases and weak acids will be investigated in order to better understand the nitrosyl reduction mechanism.

## Experimental Section

**Equipment.** The voltammetric data were obtained with an IBM EC/225 voltammetric analyzer and a Hewlett-Packard 7045A X-Y recorder. A three-electrode IBM cell was used for voltammetry, which consisted of a platinum working and auxiliary electrode and a Ag/0.1 M $AgNO_3$ in acetonitrile or an aqueous saturated calomel (SCE) reference electrode. Low temperatures were achieved with a water/alcohol/dry ice bath. The visible spectra were obtained on a Perkin-Elmer 320 UV/visible spectrophotometer with a Perkin-Elmer 3600 data station. A Dewar flask was constructed with a 1-cm visible cell that was incorporated in the flask for low-temperature spectroscopy. An OTTLE cell[13] was used for the visible spectroelectrochemical experiments. The resonance Raman data were obtained on a Spex 1877 Triplemate or a Spex 1403 spectrometer. The detector for the Triplemate spectrometer

*To whom correspondence should be addressed.

(1) Hirasawa, M.; Shaw, R. W.; Palmer, G.; Knaff, D. B. *J. Biol. Chem.* **1987**, *262*, 12428.
(2) Janick, P. A.; Rueger, D. C.; Krueger, R. J.; Barber, M. J.; Siegel, L. M. *Biochemistry* **1983**, *22*, 396.
(3) Fry, I. V.; Cammack, R.; Hucklesby, D. P.; Hewitt, E. J. *FEBS Lett.* **1980**, *111*, 377.
(4) Christner, J. A.; Janick, P. A.; Siegel, L. M.; Munck, E. *J. Biol. Chem.* **1983**, *258*, 11157.
(5) Chang, C. K. In *The Biological Chemistry of Iron. A Look at the Metabolism of Iron and its Subsequent Uses in Living Organisms*; Dunford, H. B., Dolphin, D., Raymond, K. N., Sieker, L., Eds.; D. Reidel Publishing Co.: Dordrecht, Holland, 1982; pp 313-334.
(6) Fernandes, J. B.; Feng, D.; Chang, A.; Keyser, A.; Ryan, M. D. *Inorg. Chem.* **1986**, *25*, 2606.
(7) (a) Lancon, D.; Kadish, K. M. *J. Am. Chem. Soc.* **1983**, *105*, 5610. (b) Olson, L.; Schaeper, D.; Lancon, D.; Kadish, K. M. *J. Am. Chem. Soc.* **1982**, *104*, 2042.
(8) Fujita, E.; Fajer, J. *J. Am. Chem. Soc.* **1983**, *105*, 6743.
(9) $H_2TPP$ = tetraphenylporphyrin; $H_2OEP$ = octaethylporphyrin; $H_2OEC$ = octaethylchlorin; $H_2OEiBC$ = octaethylisobacteriochlorin.
(10) Barley, M. H.; Takeuchi, K.; Murphy, W. R., Jr.; Meyer, T. J. *J. Chem. Soc., Chem. Commun.* **1985**, 507.
(11) Barley, M. H.; Takeuchi, K. J.; Meyer, T. J. *J. Am. Chem. Soc.* **1986**, *108*, 5876.
(12) Choi, I.-K.; Ryan, M. D. *Inorg. Chim. Acta* **1988**, *153*, 25.
(13) Lin, X. Q.; Kadish, K. M. *Anal. Chem.* **1985**, *57*, 1498.

0020-1669/91/1330-1832$02.50/0 © 1991 American Chemical Society

**Table I.** Visible Spectral Data for Fe(P)(NO) Complexes and Their Reduction Products

| complex | solvent | method[a] | visible bands, nm ($10^{-3}\epsilon$)[b] | ref |
|---|---|---|---|---|
| Fe(TPP)(NO) | THF | | 408 (115), 536 (9.5), 607 (2.6) | tw[c] |
| | PhCN | | 410 (110), 540 (9), 610 (4) | 7 |
| $Fe(TPP)(NO)^-$ | THF | NaAn | 406, 513, 614 | tw |
| | THF | OTTLE | 408 (101), 516 (11), 614 (3.5) | tw |
| | THF | $(TBA)(BH_4)$ | 408 (106), 516 (11), 614 (2.6) | tw |
| | PhCN | OTTLE | 414 (110), 517 (11), 539 sh, 619 (3.6) | 7 |
| $Fe(TPP)(NO)^{2-}$ | THF | OTTLE | 452 (67), 545 (19) | tw |
| Fe(TPC)(NO) | THF | OTTLE | 409 (103), 541 (8.0), 619 (13) | tw |
| $Fe(TPC)(NO)^-$ | THF | OTTLE | 406 (88), 504 (10), 546 (11), 621 (16) | tw |
| $Fe(TPC)(NO)^{2-}$ | THF | OTTLE | 409 (55), 567 (16) | tw |
| Fe(OEP)(NO) | THF | | 389 (90), 477 (13), 541 (12), 555 (12) | tw |
| | PhCN | | 394 (84), 481 (12.6), 530 (12), 552 (11.4) | 7 |
| $Fe(OEP)(NO)^-$ | THF | NaNp | 389, 538 | tw |
| | PhCN | OTTLE | 389, 537 | 8 |
| | PhCN | OTTLE | 394 (84), 541 (26), 581 (8.2) | 7 |
| | THF | OTTLE | 389 (85), 541 (22) | tw |
| $Fe(OEP)(NO)^{2-}$ | THF | OTTLE | 393 (49), 433 sh, 543 (15), 571 s | tw |

[a] Reduction method: NaAn = sodium anthracenide, NaNp = sodium naphthalenide, OTTLE = optically transparent thin-layer electrochemical cell. [b] sh = shoulder. [c] tw = this work.

was a Tracor-Northern TN6100 photodiode array detector, while the Spex 1403 spectrometer had a photomultiplier detector. The laser source was a Coherent Innova 100 or a Spectra-Physics 146 $Kr^+$ laser (406.7 nm).

**Chemicals.** Tetraphenylporphyrin ($H_2TPP$), octaethylporphyrin ($H_2OEP$), and tetrabutylammonium hydroxide ((TBA)(OH)) were purchased from Aldrich Chemical Co. Tetraphenylchlorin, Fe(TPC)Cl, Fe(OEP)(NO), and Fe(TPP)(NO) were synthesized by using literature procedures.[14-17] Tetrabutylammonium perchlorate (TBAP) was obtained from GFS Chemical Co. Tetrabutylammonium tetrahydroborate ($(TBA)(BH_4)$) was purchased from Alfa Products. Sodium anthracenide (NaAn) and sodium naphthalenide (NaNp) were generated by literature methods.[18]

Tetrahydrofuran (THF) was purified by heating at reflux over potassium under an argon atmosphere until the blue benzophenone radical color was persistent. The solvent was then distilled and transferred to a storage bottle under argon. The purified solvent was stored in a glovebox until used. Methylene chloride was purified by heating at reflux over calcium hydride, followed by distillation.

**Procedures.** The voltammetric solutions were degassed with prepurified dinitrogen that had been saturated with the solvent. The analyses of gaseous reaction products except for ammonia were performed by using a Gow-Mac 580 gas chromatograph. The determination of dihydrogen was carried out on a 5-Å molecular sieve column (Alltech 5605PC) with dinitrogen as the carrier gas and a thermal conductivity detector.[19] Gas samples were withdrawn from an enclosed container by using a gas syringe. The analysis of nitrous oxide was carried out on a Porapak Q column (Alltech 2701PC).

A mercury-pool electrode was used for coulometric reductions. The platinum-flag counter electrode was separated from the electrolysis solution with a sintered-glass frit. For the analyses of gaseous products, the solution was degassed with helium and 6–7 mg of Fe(P)(NO) was added. For experiments that involved the analyses of nitrous oxide or hydroxylamine, 5 mL of THF was placed in a side-arm flask. The electrolysis vessel was sealed to prevent exchange of gases with the outside, and the electrolysis was carried out. After the electrolysis, the system was allowed to stand so that the nitrous oxide and dinitrogen vapors would equilibrate between the electrolysis solution and the side-arm flask.[20] From the side-arm flask was removed by syringe 100 μL of solution for gas chromatographic analysis, as well as 200 μL of the gas phase. The concentration of nitrous oxide or dinitrogen can be determined from either sample by using nitrous oxide or dinitrogen standards, respectively. Once the nitrous oxide or dinitrogen concentrations had been determined, the electrolysis solution was purged with helium, and the ammonia was trapped with 4.0 mL of 0.01 M HCl. After the purging was complete, 3.0 mL of cold alkaline phenol and 1.5 mL of chlorine solution were added, and the mixture was shaken well and placed in a 100 °C water bath for 2 min.[20,21] The chlorine solution was generated by the decomposition of calcium hypochlorite in potassium carbonate. The concentration of ammonia was then determined from the visible absorbance at 636 nm. At higher concentrations of phenol, ammonia was retained in the electrolysis solution due to the formation of ammonium ion. The partitioning between ammonia and ammonium was determined from standard ammonia solutions at each phenol concentration. The presence of hydroxylamine was determined by decomposing any hydroxylamine present to nitrous oxide with ferric sulfate. The nitrous oxide generated was measured as above. Standards for dinitrogen, ammonia, nitrous oxide, and hydroxylamine were determined under conditions that duplicated those for the reaction solutions.

## Results

**Voltammetry of Fe(P)(NO).** The polarographic reduction of Fe(TPP)(NO) in THF was carried out to more negative potentials than previously reported,[7] and three one-electron waves, with $E_{1/2}$ values of −0.92, −1.75, and −2.18 V vs SCE, were observed. The first two waves were reversible in polarography and cyclic voltammetry. The stability of $Fe(TPP)(NO)^{2-}$, as monitored by the anodic peak current of the second wave, was much greater in THF than was seen earlier in methylene chloride.[7] The third wave was irreversible in cyclic voltammetry, but the polarographic log (slope) value was still 60, indicating a reversible electron transfer with an irreversible chemical reaction. The products of the first two waves can be written as $Fe(TPP)(NO)^-$ and $Fe(TPP)(NO)^{2-}$. The visible spectrum of $Fe(TPP)(NO)^-$, obtained with an optically transparent thin-layer electrochemical (OTTLE) cell, was consistent with previously reported spectra[7,8] (Table I). Reversal of the potential led to the regeneration of Fe(TPP)(NO), indicating that the one-electron-reduction product was stable on the time scale of this experiment. Reduction of Fe(TPP)(NO) at a potential corresponding to the second wave generated $Fe(TPP)(NO)^{2-}$ (Figure 1). As with $Fe(TPP)(NO)^-$, the reaction was reversible and reversal of the potential generated $Fe(TPP)(NO)^-$ and, finally, Fe(TPP)(NO), indicating that no decomposition of the iron–nitrosyl complex occurred. Similar results could be obtained for Fe(TPC)(NO) and Fe(OEP)(NO) (Table I).

**Generation of $Fe(P)(NO)^-$.** It had been observed earlier that the coulometric reduction of Fe(TPP)(NO) in methylene chloride did not lead to the generation of $Fe(TPP)(NO)^-$, but a catalytic reaction occurred that led to the regeneration of Fe(TPP)(NO).[7b,8] This was also observed in our work for the first 1–2 equiv of electrons. Further electrolysis led to the appearance of a new spectrum that was identical with that of $Fe(TPP)(OH)^-$ (Figure 2), which was verified by adding (TBA)(OH) to a solution of $Fe^{II}(TPP)$. The mechanism for the formation of this complex will

(14) Whitlock, H. W.; Hanauer, J. R.; Dester, M. Y.; Bower, B. K. *J. Am. Chem. Soc.* **1967**, *91*, 7495.
(15) Feng, D.; Ting, Y.-S.; Ryan, M. D. *Inorg. Chem.* **1985**, *24*, 612.
(16) Alder, A. D.; Longo, F. R.; Finarelli, J. D.; Goldmacher, J.; Assour, J.; Korsakoff, L. *J. Org. Chem.* **1967**, *32*, 467.
(17) Wayland, B. B.; Olson, L. W. *J. Am. Chem. Soc.* **1974**, *96*, 6037.
(18) Hickman, D. L.; Shirazi, A.; Goff, H. M. *Inorg. Chem.* **1985**, *24*, 563.
(19) Jeffery, P. G.; Kipping, P. J. *Gas Analysis by Gas Chromatography*, 2nd ed.; Pergamon Press: Oxford, U.K., 1972; p 88.
(20) Conway, E. J. *Microdiffusion Analysis and Volumetric Error*, 5th ed.; C. Lockwood: London, 1962.
(21) Russell, J. A. *J. Biol. Chem.* **1945**, *156*, 457.
(22) Rao, K. B.; Rao, G. G. *Z. Anal. Chem.* **1942**, *64*, 731.

**Table II.** Resonance Raman Vibrations of Iron Porphyrins ($cm^{-1}$)

| complex | solvent | oxid/spin state | $\nu_2$ | $\nu_4$ | $\nu_{NO}$ | $\nu_{Fe-NO}$ | ref |
|---|---|---|---|---|---|---|---|
| Fe(TPP)($^{14}$NO) | THF | +2/l.s. | 1564 | 1366 | 1681 | 525 | tw[a] |
| Fe(TPP)($^{15}$NO) | THF | +2/l.s. | 1564 | 1366 | 1647 | 517 | tw |
| Fe(TPP)($^{14}$NO)$^-$ | THF | +2/l.s. | 1561 | 1366 | 1496 | 549 | tw |
| Fe(TPP)($^{15}$NO)$^-$ | THF | +2/l.s. | 1561 | 1366 | 1475 | 538 | tw |
| Fe(TPP)(NO) | $CHCl_3$ | +2/l.s. | 1567 | 1368 | | | 23 |
| Fe(TPP) | $CH_2Cl_2$ | +2/i.s. | 1565 | 1370 | | | 24 |
| Fe(TPP) | DMF | +2/h.s. | 1540 | 1344 | | | 25 |
| Fe(TPP) | THF | +2/h.s. | 1540 | 1345 | | | tw |
| Fe(TPP)(OH)$^-$ | THF | +2/h.s. | 1546 | 1360 | | | tw |
| Fe(TPP)(1-MeIm)$_2$ | $CH_2Cl_2$ | +2/l.s. | 1557 | 1354 | | | 24 |
| Fe(TPP)$^-$ | DMF | +1/l.s. | 1554 | 1356 | | | 25 |
| Fe(TPP)Cl | $CH_2Cl_2$ | +3/h.s. | 1555 | 1366 | | | 24 |
| Fe(TPP)(DMF)$_2^+$ | DMF | +3/h.s. | 1553 | 1360 | | | 26 |
| Fe(TPP)(Im)$_2^+$ | $CH_2Cl_2$ | +3/l.s. | 1568 | 1370 | | | 24 |

[a] tw = this work.

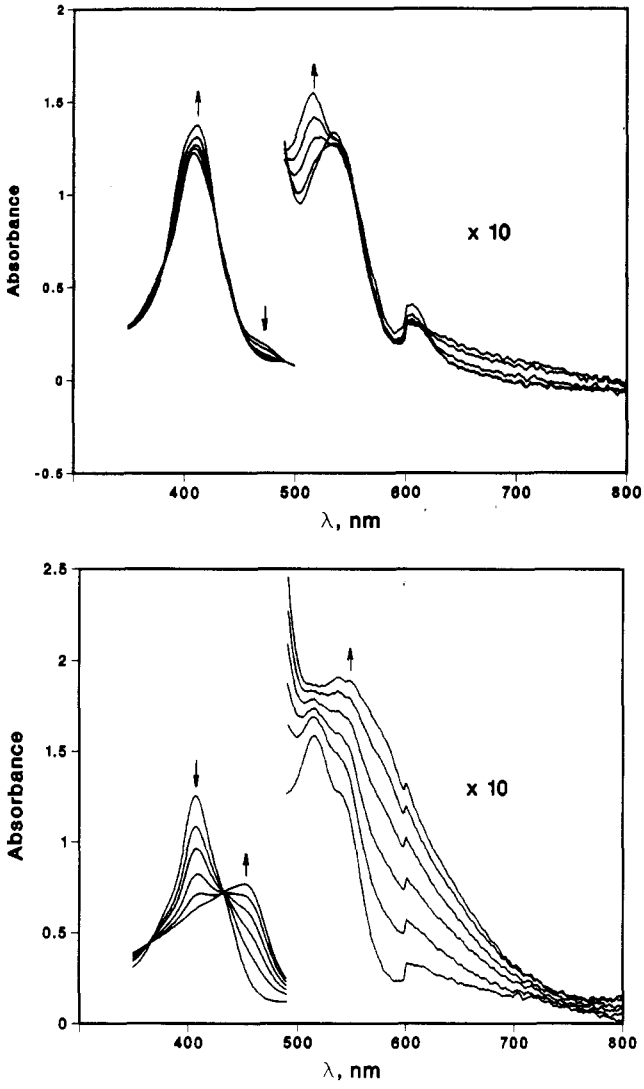


**Figure 1.** OTTLE spectroelectrochemical spectra: (A, top) reduction of Fe(TPP)(NO) to form Fe(TPP)(NO); (B, bottom) reduction of Fe(TPP)(NO)$^-$ to form Fe(TPP)(NO)$^{2-}$. Solvent is THF. Arrows indicate the spectral changes as the potential is stepped more negatively.

be discussed later. Unlike the situation observed in methylene chloride, Fe(TPP)(NO)$^-$ was much more stable in THF, and it was possible to coulometrically reduce iron porphyrin nitrosyls quantitatively in this solvent. The anionic products were stable indefinitely as long as oxygen and water was excluded.

Similar results were also observed for the chemical reduction of Fe(TPC)(NO) and Fe(OEP)(NO). In THF, borohydride, sodium naphthalenide, or sodium anthracenide could be used to generate quantitatively Fe(P)(NO)$^-$. The spectra that were obtained by these chemical and coulometric methods were consistent with the spectroelectrochemical data (Table I). While the product was stable in THF, the one-electron-reduced product could only be obtained in methylene chloride at reduced temperatures (0 °C or less). Even under these conditions, though, the product was not indefinitely stable and slowly decomposed within $^1/_2$–1 h.

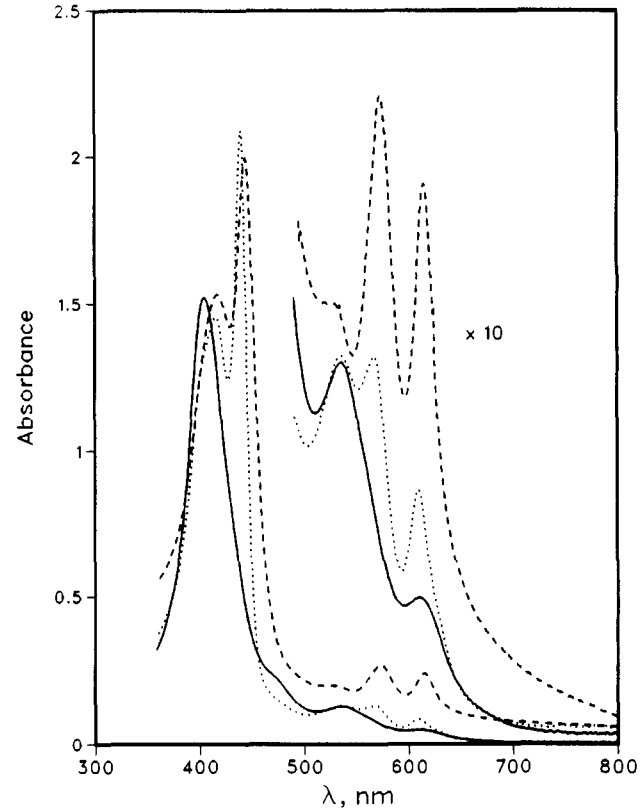


**Figure 2.** Visible spectra of the product formed by the coulometric reduction of Fe(TPP)(NO) in methylene chloride: solid line, before electrolysis; dotted line, after 2.6 equiv of electrons. The dashed line shows the visible spectrum of Fe(TPP)(OH)$^-$ formed by the reaction of Fe(TPP) with (TBA)(OH).

**Spectroscopic Studies of Fe(TPP)(NO) and Its Reduction Products.** For stability reasons, most of the spectral and chemical studies of Fe(P)(NO)$^-$ were carried out in THF. The resonance Raman spectra of Fe(TPP)(NO), for $^{14}$NO and $^{15}$NO, were obtained in THF (Figure 3). Some selected bands are shown in Table II. The spectra were consistent with previous work in chloroform[23] (see Table II), except that the N–O stretching

(23) Chottard, G.; Battioni, P.; Battioni, J.-P.; Lange, M.; Mansuy, D. *Inorg. Chem.* **1981**, *20*, 1718.
(24) Burke, J. M.; Kincaid, J. R.; Peters, S.; Gagne, R. R.; Collman, J. P.; Spiro, T. G. *J. Am. Chem. Soc.* **1978**, *100*, 6083.
(25) Donohoe, R. J.; Atamian, M. A.; Bocian, D. F. *J. Am. Chem. Soc.* **1987**, *109*, 5593.

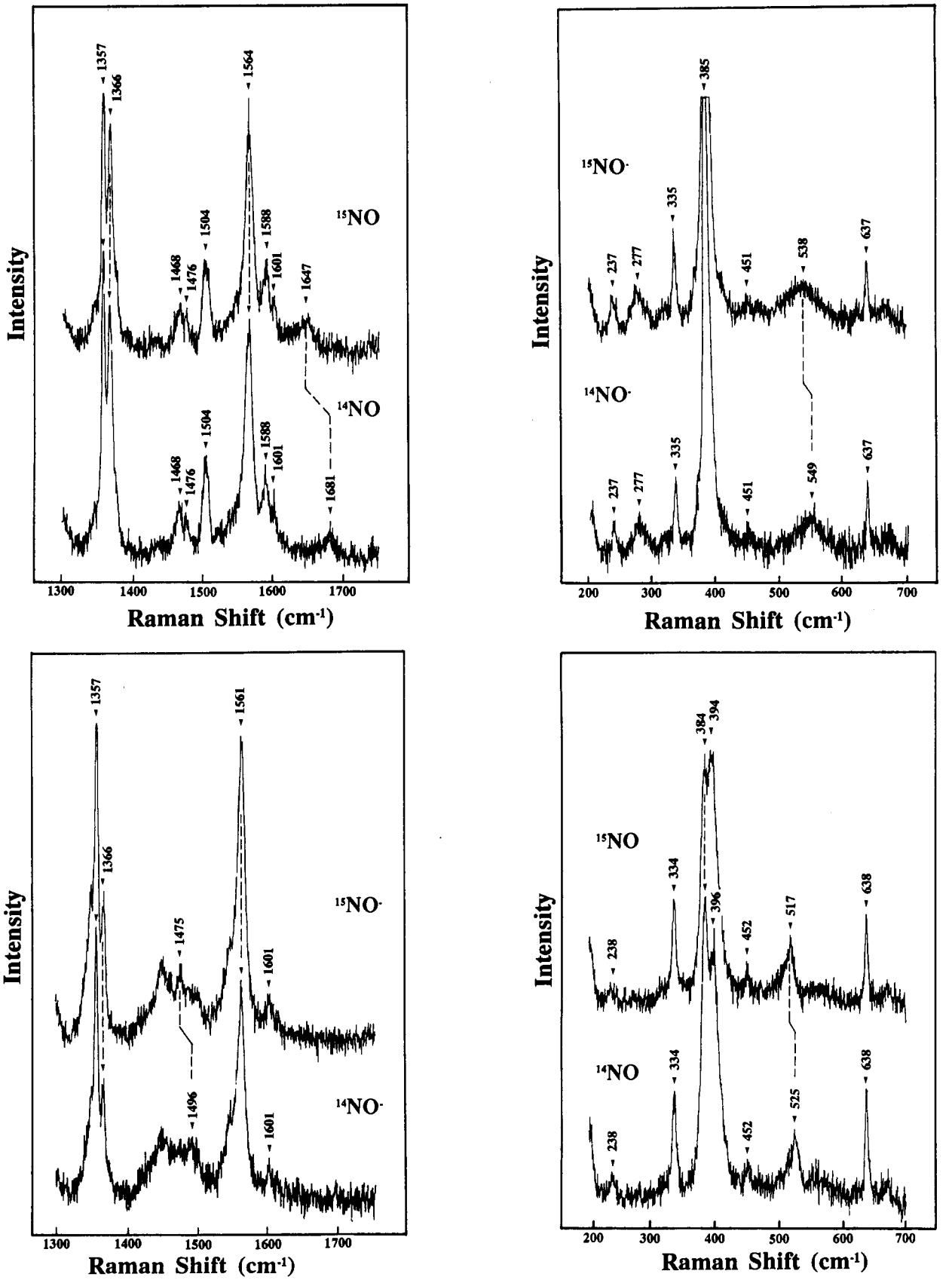


**Figure 3.** Resonance Raman spectra: (A, top left) Fe(TPP)(NO), high-energy region; (B, bottom left) Fe(TPP)(NO)$^-$, high-energy region; (C, top right) Fe(TPP)(NO), low-energy region; (D, bottom right) Fe(TPP)(NO)$^-$, low-energy region. All spectra were recorded in THF with Soret excitation.

frequency was not previously observed. Under our conditions in THF, though, this band could be observed at 1681 cm$^{-1}$. Upon $^{15}$N isotopic substitution of the NO, the frequency of this band decreased to 1647 cm$^{-1}$. A second band, sensitive to $^{15}$N substitution, was observed at 525 cm$^{-1}$, which decreased to 517 cm$^{-1}$ with $^{15}$NO.

The resonance Raman spectrum of Fe(TPP)(NO)$^-$ was obtained by using electrochemical reduction at a platinum electrode (Figure 3). Significant changes in the resonance Raman spectrum

(26) Mashiko, T.; Kastner, M. E.; Spartalian, K.; Scheidt, W. R.; Reed, C. A. *J. Am. Chem. Soc.* **1978**, *100*, 6345.

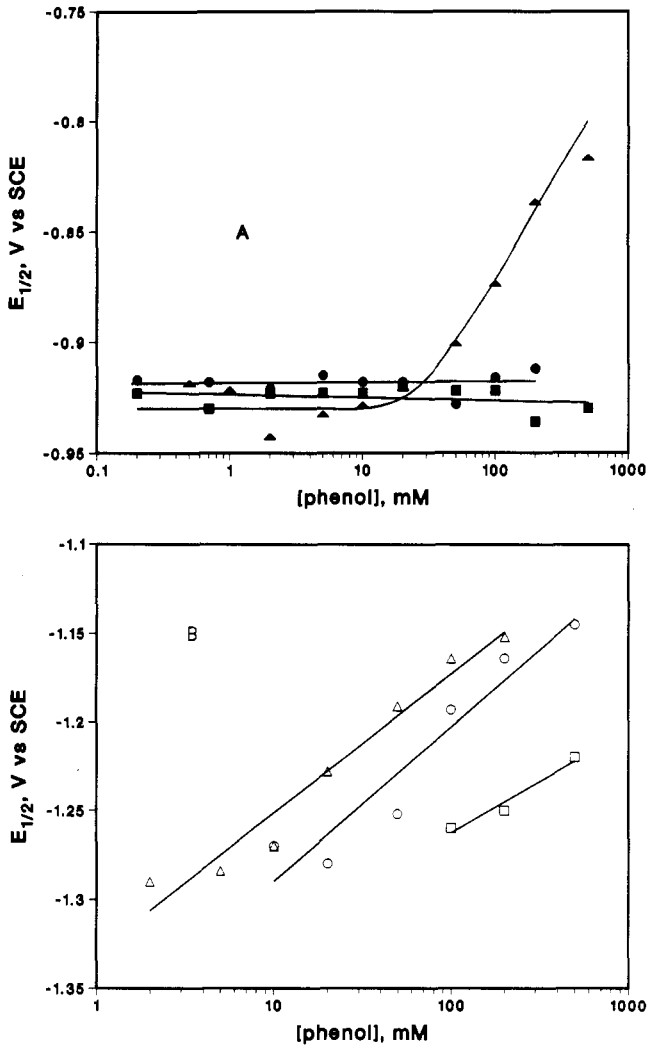


**Figure 4.** Variation in the polarographic half-wave potentials for the first (A) and second (B) waves of Fe(TPP)(NO) as a function of the concentrations of phenol (□), 2-chlorophenol (○), and 2,3-dichlorophenol (▲). Solid symbols are for the first wave, and the open symbols are for the second wave. Conditions: solvent THF; electrolyte TBAP; dropping mercury electrode; 23 °C.

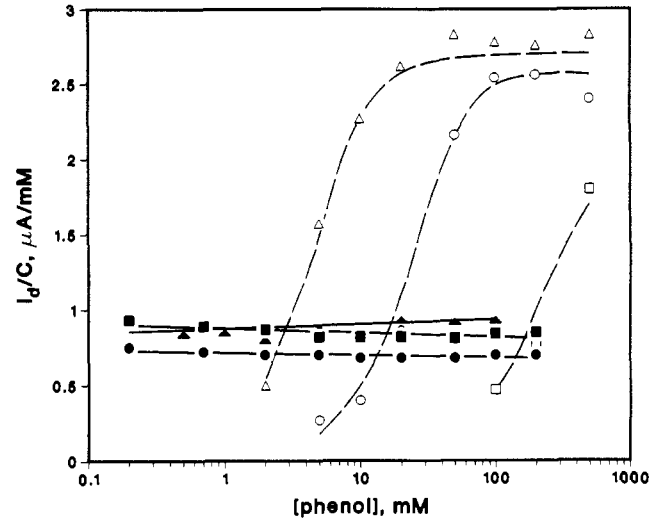


**Figure 5.** Variation in the limiting currents for the first (solid line) and second (dashed line) waves of Fe(TPP)(NO) as a function of the concentration of phenol (□), 2-chlorophenol (○), and 2,3-dichlorophenol (▲). Solid symbols are for the first wave, and open symbols are for the second wave. The solid lines are drawn from the least-squares-fit line. Conditions: solvent THF; electrolyte TBAP; dropping mercury electrode; 23 °C.

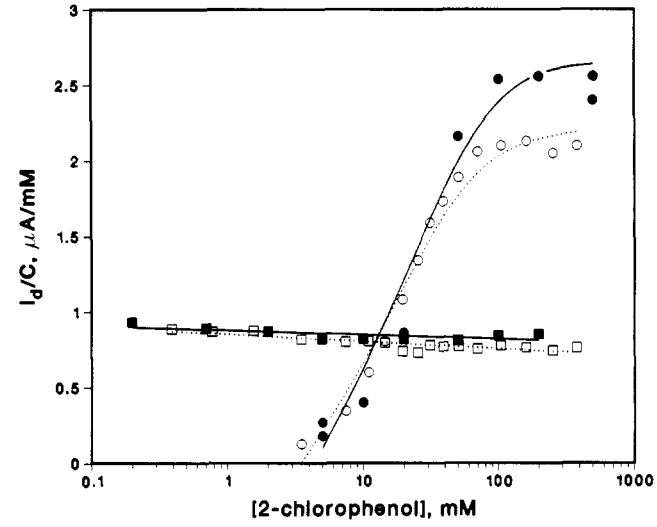


**Figure 6.** Variation in the polarographic limiting currents of waves I (squares) and IIb (circles) for Fe(TPP)(NO) (solid line, solid symbols) and Fe(TPC)(NO) (dotted line, open symbols) as a function of the concentration of 2-chlorophenol in THF. Conditions: electrolyte TBAP; dropping mercury electrode.

occurred. The band associated with the N–O stretch disappeared upon reduction, and a new, weak but reproducible, band appeared at 1496 $cm^{-1}$. Repetition of this experiment with Fe(TPP)($^{15}$NO) caused the 1496-$cm^{-1}$ band to shift to 1475 $cm^{-1}$. The low-energy region, though, was much more informative (Figure 3). Reduction of Fe(TPP)($^{14}$NO) caused the band at 525 $cm^{-1}$ to disappear and a new band at 549 $cm^{-1}$ to appear. This new band was also sensitive to isotopic substitution and decreased to 538 $cm^{-1}$ in Fe(TPP)($^{15}$NO)$^-$.

Reoxidation of Fe(TPP)(NO)$^-$ regenerated the original Fe(TPP)(NO) spectrum, indicating that photolysis or other decomposition processes were not important. Care was taken in carrying out this experiment to minimize any photochemical decomposition of the nitrosyl complexes. Low laser powers, short acquisition times, and stirred solutions were used to prevent photolysis. When photolysis occurred, Fe(TPP), which would give rise to a distinctive resonance Raman spectrum (e.g., bands at 1345 and 1540 $cm^{-1}$), was observed. In addition, no bands for Fe(TPP)(OH)$^-$ (1360 and 1546 $cm^{-1}$) appeared, indicating that, under dry conditions, iron(II) hydroxide was not formed. This was also consistent with the visible spectrum. Chemical reduction of Fe(TPP)(NO) with NaAn gave a spectrum identical with that of Fe(TPP)(NO)$^-$, but with a high background due to anthracene fluorescence.

**Polarography and Coulometry of Fe(P)(NO) in the Presence of Phenols.** The generation of ammonia from NO must occur by a series of electron transfer/protonation steps. In order to examine this reaction mechanism, the dc polarography of Fe(TPP)(NO) was carried out in the presence of weak acids such as substituted phenols. The first wave (wave I) was relatively unaffected by 2-chlorophenol, while a new second wave (wave IIb) appeared between the first wave (wave I) and the original second wave (wave IIa). The variations in the half-wave potentials and limiting currents for the first (wave I) and the new second wave (wave IIb) as a function of the concentration of phenol are shown in Figures 4 and 5. The half-wave potential (except for high acid concentrations) and the limiting current of wave I were independent of the concentration of the weak acid. By contrast, the position and height of wave IIb were strongly affected by the presence of substituted phenols.

For the two strongest acids studied, the limiting current of wave IIb leveled off at a value that corresponded to a three-electron wave. Phenol, itself, was a too weak acid for the limiting current of wave IIb to reach three electrons. Finally, the stronger the acid (as measured by its $pK_a$), the lower the concentration of the substituted phenol that was necessary for the appearance of wave IIb. In addition, there was no difference observed between the

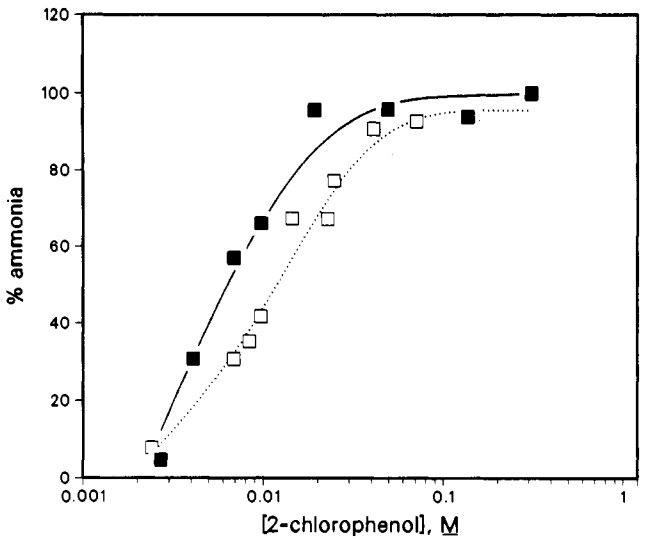


**Figure 7.** Variation in the yield of ammonia in the electrolysis of Fe(TPP)(NO) (solid line, solid squares) and Fe(TPC)(NO) (dotted line, open squares) as a function of the concentration of 2-chlorophenol in THF. A mercury-pool cathode was used.

chlorin or porphyrin macrocycle in the half-wave potential or limiting current of wave IIb for a given concentration of an acid (see Figure 6).

The electrolyses of Fe(TPP)(NO) and Fe(TPC)(NO) in the presence of 2-chlorophenol were carried out at a potential that corresponded to the limiting current of the second wave, and the product concentrations were determined. The results are shown in Figure 7. Above 20 mM 2-chlorophenol, the yield of ammonia was about 90–100%. No detectable amounts of nitrous oxide, dinitrogen, or hydroxylamine were observed. Previous studies in this laboratory have shown that hydroxylamine is not stable in the presence of iron porphyrins, rapidly disproportionating to yield ammonia and Fe(P)(NO).[27] The nitrosyl formed by the reductive nitrosylation may be further reduced. Unlike the polarographic study, there was a small difference in ammonia yields between using porphyrin and using chlorin as the macrocycle. Somewhat higher concentrations of 2-chlorophenol were needed for Fe(TPC)(NO) to generate the same yield of ammonia as Fe(TPP)(NO). For both macrocycles though, nearly quantitative yields were obtained with sufficient concentrations of 2-chlorophenol.

**Reaction of Fe(P)(NO)$^-$ with Phenols.** Fe(TPP)(NO)$^-$ and Fe(OEP)(NO)$^-$ were generated in THF by the chemical reduction of their respective nitrosyls with borohydride or sodium anthracenide. Degassed phenol or a substituted phenol was added to these solutions by a syringe. The visible spectra were obtained before and after the addition of phenol. For both porphyrins, the original nitrosyl complex, Fe(P)(NO), was regenerated with no evidence for the reduction of the coordinated nitrosyl. The following mechanism can be written for the reaction of phenol with the reduced nitrosyl:

$$Fe(P)(NO)^- + PhOH \rightarrow Fe(P)(NO) + PhO^- + \tfrac{1}{2}H_2 \qquad (1)$$

This reaction is thermodynamically favorable, and polarography can be carried out only because of the large overpotential for hydrogen evolution on mercury. Further confirmation of this reaction was obtained by gas chromatographic head-space analysis. The addition of 2-chlorophenol to a solution of Fe(TPP)(NO)$^-$ generated 1 equiv of $H_2$ (based on reducing agent), as would be expected from the above reaction. Substoichiometric amounts of borohydride were used to prevent direct reduction of the reducing agent with phenol. No changes were observed in the visible spectrum when Fe(P)(NO) and 2-chlorophenol were mixed.

**Reactions of Fe(P)(NO) and Fe(P)(NO)$^-$ with Hydroxide.** In addition to phenols, Fe(TPP)(NO)$^-$ was also found to react with hydroxide. While no changes were observed in the visible spectrum of Fe(TPP)(NO) when hydroxide ion (as (TBA)(OH)) was added, significant spectral changes were seen when hydroxide was added to Fe(TPP)(NO)$^-$. The visible spectrum of Fe(TPP)(OH)$^-$ appeared rapidly, and the reduced nitrosyl spectra completely disappeared. The following mechanism is consistent with these results:

$$Fe(P)(NO)^- + OH^- \rightarrow Fe(P)(OH)^- + NO^- \qquad (2)$$

We did not investigate the fate of $NO^-$, but it is known that this radical species will rapidly dimerize to form $N_2O_2^{2-}$.

## Discussion

**Resonance Raman Spectra of Fe(TPP)(NO).** The porphyrin vibrations of Fe(TPP)(NO) in THF were consistent with previous studies in chloroform.[23] While the N–O stretching and Fe–NO bands were not observed for five-coordinate Fe(P)(NO) complexes in chloroform,[28] we were able to observe both bands in THF. The shift in frequency of 34 cm$^{-1}$ for $\nu_{NO}$ upon isotopic substitution of the nitrogen is within the range predicted on the basis of the mass change (a shift of 30 and 37 cm$^{-1}$ was observed for nitrosylhemoglobin and nitrosylmyoglobin, respectively[29]). Similarly, an Fe–NO band was observed at 525 cm$^{-1}$, which decreased to 517 cm$^{-1}$ with $^{15}NO$. This compares with the correspondent vibration in ferrous nitrosylhemoglobin (six-coordinate), which was observed at 553 cm$^{-1}$ [30,31] and decreased by 7 cm$^{-1}$ with $^{15}NO$.[30] It is not clear at this time whether the band is an Fe–N–O stretching or bending vibration.[32]

**Characterization of Fe(TPP)(NO)$^-$.** Two bands were observed for Fe(TPP)(NO)$^-$ that were sensitive to $^{15}NO$ substitution: a very weak band at 1496 cm$^{-1}$ ($\nu_{NO}$) and a stronger band at 549 cm$^{-1}$. The appearance of the Fe–NO vibration provides unequivocal evidence for the fact that the nitrosyl group has remained coordinated to the iron, as well as the fact that Fe(TPP)(NO) can be regenerated upon reoxidation. The $\nu_{NO}$ band decreased from 1681 to 1496 cm$^{-1}$ (or 185 cm$^{-1}$), while the Fe–NO band increased from 525 to 549 cm$^{-1}$ (24 cm$^{-1}$), upon reduction. Infrared studies of coordinated $NO^-$ complexes have shown that $\nu_{NO}$ should be in the region from about 1500 to 1750 cm$^{-1}$.[33] Upon substitution with $^{15}NO$, these two bands decreased to 1475 and 538 cm$^{-1}$, respectively. For the Fe–NO band, the shift of 11 cm$^{-1}$ is consistent with previous work (see above), and the $\nu_{NO}$ shift of 21 cm$^{-1}$ is in reasonable agreement with the predicted shift of 27 cm$^{-1}$.

An examination of the porphyrin vibrations of Fe(TPP)(NO)$^-$ showed small, but identifiable, differences with Fe(TPP)(NO) and significant differences with Fe(TPP)(OH)$^-$ and Fe(TPP) (see Table II). The $\nu_2$ decreased from 1564 to 1561 cm$^{-1}$ upon reduction. Previous work has shown that a vibration around 1564 cm$^{-1}$ was indicative of a low-spin ferrous complex. This value is significantly different from the $\nu_2$ band in Fe(TPP) in THF (high spin), which has a value of 1540 cm$^{-1}$. In particular, one could observe Fe(TPP) if the laser beam was too intense and photolytically cleaved NO from the iron complex. By contrast, the low-spin Fe$^I$(TPP) complex in DMF has a $\nu_2$ value of 1554 cm$^{-1}$.[25] Ring-centered reductions can be distinguished from metal-centered (or ligand-centered) reductions on the basis of $\nu_2$.[25] Reduction of Zn(TPP) to form Zn(TPP)$^-$ gave rise to a significant decrease in $\nu_2$ from 1548 to 1531 cm$^{-1}$, while little change was observed in the formation of Fe$^I$(TPP).[25,34] Similar results were observed

(27) Feng, D.; Ryan, M. D. *Inorg. Chem.* **1987**, *26*, 2480.

(28) Tsubaki, M.; Yu, N.-T. *Biochemistry* **1982**, *21*, 1140.
(29) Mackin, H. C.; Benko, B.; Yu, N.-T.; Gersonde, K. *FEBS Lett.* **1983**, *158*, 199.
(30) Stong, J. D.; Burke, J. M.; Daly, P.; Wright, P.; Spiro, T. G. *J. Am. Chem. Soc.* **1980**, *102*, 5815.
(31) Chottard, G.; Mansuy, D. *Biochem. Biophys. Res. Commun.* **1977**, *77*, 1333.
(32) Benko, B.; Yu, N.-T. *Proc. Natl. Acad. Sci. U.S.A.* **1983**, *80*, 7042.
(33) Snyder, D. A.; Weaver, D. L. *Inorg. Chem.* **1970**, *9*, 2760.
(34) Ksenofontova, N. M.; Maslov, V. G.; Sidorov, A. N.; Bobovich, Ya. S. *Opt. Spectrosc. (Engl. Transl.)* **1976**, *40*, 462.

for the $\nu_4$ band. There was no change in the $\nu_4$ band when Fe(TPP)(NO) was reduced (1366 $cm^{-1}$), and this band was identical with that of the complex $Fe(TPP)(O_2)$,[35] which is isoelectronic with $Fe(TPP)(NO)^-$. By contrast, this band for Fe(TPP) in THF occurs at 1345 $cm^{-1}$ and for $Fe(TPP)^-$ in DMF occurs at 1356 $cm^{-1}$.[25]

On the basis of molecular orbital diagram of Waleh et al.,[36] the additional electron should fill a half-filled orbital in Fe(TPP)(NO), which is 61% NO $\pi^*$, 26% NO $\sigma$, and 7% $d_{\pi}$. Because this orbital came from a $\pi^*$ orbital in NO, addition of an electron will significantly weaken the N–O bond and strengthen the Fe–N bond. The resonance Raman data are consistent with such a result. In summary, $Fe(TPP)(NO)^-$ appears to be a low-spin ferrous complex with a coordinated $NO^-$ ligand.

While only visible spectral information was obtained for $Fe(P)(NO)^{2-}$, formation of this species led to attenuation of the Soret band, an effect similar to what was observed in $Fe(P)^-$, but not nearly as pronounced. Resonance Raman spectroscopy of $Fe(P)(NO)^{2-}$ has not been successful yet due to a weak resonance Raman signal (due to a weaker absorber), poor stability of $Fe(P)(NO)^{2-}$, and photodissociation of the nitrosyl complex in the OTTLE cell that was used (the OTTLE cell allows the more rapid generation of $Fe(P)(NO)^{2-}$ in order to overcome the problem of limited stability).

**Polarography of Fe(TPP)(NO) in the Presence of Phenol.** The addition of substituted phenols had little or no effect on the position and limiting current for the first reduction wave of Fe(TPP)(NO). The only observed effect on this wave was a positive shift in the $E_{1/2}$ when high concentrations of phenols were used. Thus, on the polarographic time scale, addition of a weak acid did not lead to multielectron reductions at the first wave, and hence, an ECE, disproportionation, or catalytic mechanism was not observed. Only on the longer time scale could the indirect reduction of a weak acid to form dihydrogen (reaction 1) be observed. Reaction 1, with the subsequent reduction of Fe(P)(NO), would give rise to a classical catalytic mechanism, which would require an increase in the limiting current. These results indicate that $Fe(P)(NO)^-$ is a weak base and that the protonated complex is probably more difficult to reduce than the original nitrosyl. If the protonated nitrosyl complex were easier to reduce than Fe(P)(NO), then the addition of a weak acid should have led to reduction of the nitrosyl rather than dihydrogen, because the excess $Fe(P)(NO)^-$ would have reduced the protonated complex as follows:

$$Fe(P)(NO)^- + PhOH \rightarrow Fe(P)(NOH) + PhO^- \quad (3)$$

Once the complex is protonated, two pathways can be envisioned: either a disproportionation to form Fe(P)(NO) and dihydrogen

$$2Fe(P)(NOH) \rightarrow 2Fe(P)(NO) + H_2 \quad (4)$$

or a cross-reaction to reduce the protonated nitrosyl

$$Fe(P)(NOH) + Fe(P)(NO)^- \rightarrow Fe(P)(NOH)^- + Fe(P)(NO) \quad (5)$$

If a Fe(P)(NOH) were more difficult to reduce than Fe(P)(NO), then reaction 5 would be thermodynamically unfavorable and reaction 4 would dominate. An examination of the molecular orbital diagrams in refs 17 and 36 provides a rationale for the higher reduction potential of Fe(P)(NOH) compared to Fe(P)(NO). The first electron added to Fe(P)(NO) is added to a half-filled orbital, while the next electron must be placed in the next higher energy molecular orbital, which is empty. Even with the removal of the Coulombic effects by protonation, additional energy is still required to add the second electron. The polarography of Fe(TPP)(NO) in the presence of all three phenols was consistent with such a formulation because the first wave was always a one-electron process (Figure 5), regardless of the acid strength or concentration of the phenol. The small shift in the half-wave potential at high concentrations of phenol may be due to solvation effects or protonation, but not the further reduction of the reduced nitrosyl.

As was shown under Results, a new second wave appeared for Fe(TPP)(NO) at a potential well positive of the original second wave ($Fe(TPP)(NO)^-/Fe(TPP)(NO)^{2-}$). The limiting current for this wave was strongly dependent upon the identity and concentration of the acid. For high concentrations of chlorophenol and dichlorophenol, the limiting current leveled off at a value that corresponded to three electrons. The following reaction would be consistent with the stoichiometry of the reaction:

$$Fe(P)(NO)^- + 3e^- + 3PhOH \rightarrow Fe(P)^- + NH_2OH + 3PhO^-$$

At the potential of wave IIb, Fe(P) is not stable and will be reduced to $Fe(P)^-$. As was discussed earlier,[27] hydroxylamine will react in a reductive nitrosylation reaction to form ammonia and the nitrosyl complex. This reaction is probably too slow on the polarographic time scale (1 s) to be observed but will be important on the coulometric time scale (1 h).

The results of this work are consistent with the mechanism proposed by Barley et al.[11,37] for the electrocatalytic reduction of nitrite in water by a water-soluble iron porphyrin. In water, nitrite forms an iron–nitrosyl complex by an acid/base reaction. The wave, which corresponded to the $Fe(NO)/Fe(NO)^-$ reduction, was pH-independent except in fairly acidic solutions (pH >2.6). Under more acidic conditions, Fe(P)(NHO) (2.6 > pH > 2.1) and $Fe(P)(NH_2O^+)$ (pH <2.1) were postulated, on the basis of the $E_{1/2}$–pH curves.

**Coulometric Reduction of Fe(TPP)(NO) in Methylene Chloride.** The coulometry of Fe(TPP)(NO) in methylene chloride can be explained on the basis of the reactions of $Fe(TPP)(NO)^-$ with weak acids and hydroxide. The reaction of the reduced nitrosyl with water should be analogous to the phenol reaction.

$$Fe(TPP)(NO) + e^- \rightarrow Fe(TPP)(NO)^-$$

$$Fe(TPP)(NO)^- + H_2O \rightarrow Fe(TPP)(NO) + OH^- + \tfrac{1}{2}H_2$$

Here water is present in trace amounts in the solvent and/or electrolyte. The iron nitrosyl that is regenerated can be reduced again. Gradually the solution becomes more basic, and the hydroxide that is generated will displace $NO^-$ from the complex to form the hydroxide complex:

$$Fe(TPP)(NO)^- + OH \rightarrow Fe(TPP)(OH)^- + NO^-$$

The hydroxide complex is the ultimate product of the coulometric reduction of Fe(TPP)(NO) in methylene chloride. Because it is possible to make THF much more vigorously dry, there is no trace water available for this reaction. If the THF is not purified rigorously, the coulometric product is again $Fe(TPP)(OH)^-$.

## Conclusions

The first reduction of Fe(P)(NO) generated a low-spin ferrous complex that led to significant weakening of the NO bond and a strengthening of the Fe–N bond. The results also indicate that $Fe(P)(NO)^-$ is a surprisingly weak base, which can slowly reduce protons to dihydrogen. When proton donors, such as phenol or substituted phenols, were present, the second wave was shifted to positive potential by nearly 0.5 V. This new wave corresponded to a three-electron reduction, and on the basis of the stoichiometry of the reaction, hydroxylamine was probably formed. While the second wave was shifted to more positive potentials by the addition of weak acid, its half-wave potential remained negative of the first reduction wave. The ultimate coulometric product was ammonia. This was due to the slow reduction or the disproportionation of hydroxylamine to ammonia in the presence of iron porphyrin.[27]

All of these studies have utilized five-coordinate complexes, while the enzyme is known to be six-coordinate when substrate

(35) Wagner, W.-D.; Paeng, I. R.; Nakamoto, K. *J. Am. Chem. Soc.* **1988**, *110*, 5565.
(36) Waleh, A.; Ho, N.; Chantranupont, L.; Lowe, G. H. *J. Am. Chem. Soc.* **1989**, *111*, 2767.
(37) Because of the different stable oxidation states in water, the second and third reductions in ref 11 correspond to the first and second reductions here.

is present. The effect of coordination and porphine structure on the reduction mechanism still needs to be pursued. In addition, the study of the mechanism for the reduction of $NO^-$ to hydroxylamine and ammonia has just begun, and further work will be necessary to verify the important steps in the reduction mechanism. This work is in progress in our laboratory.

**Acknowledgment.** We thank X. Q. Lin for construction of the OTTLE cell. We also wish to acknowledge the NSF for grants for the purchase of electrochemical (PRM-8106653), spectroscopic (PRM-8201885), and Raman (CHE-8413956) equipment. In addition, we thank the Committee on Research of Marquette University for partial support of this research.

Contribution from the Department of Chemical and Biological Sciences, Oregon Graduate Institute of Science and Technology, 19600 NW von Neumann Drive, Beaverton, Oregon 97006-1999, and Department of Chemistry, University of Arizona, Tucson, Arizona 85721

# Raman-Scattering Properties of $Mo^V{=}O$ and $Mo^V{=}S$ Complexes as Probes for Molybdenum-Containing Enzymes

Gabriele Backes,[1a] John H. Enemark,[1b] and Thomas M. Loehr*,[1a]

*Received August 15, 1990*

The two monomeric Mo(V) complexes $LMoOCl_2$ and $LMoSCl_2$ having the ligand L = hydrotris(3,5-dimethyl-1-pyrazolyl)borate have been studied by Raman spectroscopy. Characteristic stretching frequencies for the $\{Mo{=}E\}^{3+}$ unit (E = O, S) in the solid state are observed at 957 $cm^{-1}$ for $\nu(Mo{=}O)$ and at 525 $cm^{-1}$ for $\nu(Mo{=}S)$. Skeletal frequencies of the remaining $\{LMoCl_2\}$ moiety are not strongly affected by substitution of an oxo versus a sulfido ligand. Enhancement profiles obtained in backscattering from solid samples of the two chromophores show the $LMoSCl_2$ compound to have a distinctive profile with maximum scattering at ~570 nm. However, the solution optical spectrum exhibits no absorption at this wavelength. The profile for the oxo analogue is rather constant in the visible range but suggests increased scattering intensity for $\nu(Mo{=}O)$ when approaching the UV region.

## Introduction

Terminal oxo groups are a characteristic property of high-valent molybdenum complexes and occur in such common cores as $\{Mo^{IV}O\}^{2+}$, $\{Mo^{V}O\}^{3+}$, $\{Mo^{VI}O_2\}^{2+}$, and $\{Mo^{VI}O_3\}$.[2] Compounds containing one or more terminal sulfido groups are also frequently seen. The $\{Mo{=}S\}$ moiety is well-known for molybdenum in the oxidation states IV and VI, but only multinuclear Mo(V)-sulfido complexes had, until recently,[3] been available.[2c,4] Mononuclear mixed oxo-sulfido Mo(VI) complexes have also been reported.[5] Molybdenum complexes containing either $\{Mo{=}S\}$ or $\{Mo{=}O\}$ have been the subject of intense spectroscopic studies since the discovery of a high-valent molybdenum center in a number of oxomolybdoenzymes.[4,6] All molybdoenzymes, except nitrogenase, possess a common molybdenum center, the Mo cofactor, that represents the enzymatically active site in these proteins.[7] This cofactor is proposed to contain a pterin ring that is chelated to the Mo atom via two sulfur atoms from a dithiolene group.[7]

A common feature of oxomolybdoenzymes is their ability to carry out an oxo-transfer reaction between the Mo center and the substrate, with Mo cycling through the oxidation states VI, V, and IV. The reactions catalyzed are formally hydroxylations of the substrate. Xanthine oxidase has been shown to contain one terminal oxo and one sulfido ligand in its resting, oxidized Mo(VI) state.[8] In the fully reduced state, the enzyme has a Mo(IV) center with one terminal oxo group. The transient Mo(V) state is believed to also contain one terminal oxo group.[8] Since X-ray crystallographic data are not yet available, the main source of information concerning the nature of the molybdenum site stems from only limited spectroscopic techniques, including EXAFS,[9,10] EPR,[11] and, potentially, NMR spectroscopy. All three oxidation states of sulfite oxidase have been studied by EXAFS,[12] but only the paramagnetic Mo(V) state can be detected by EPR spectroscopy.[11-14] $^{95}Mo$ NMR spectroscopy has proven useful in distinguishing dioxo, oxo-sulfido, and disulfido Mo(VI) complexes;[15] however, results from molybdoenzymes have not yet been realized. Thus, a considerable need for other spectroscopic probes for the molybdenum center exists.

Raman spectroscopy, especially resonance Raman spectroscopy, has proven to be a powerful technique for probing the metal sites of a variety of metalloproteins.[16] Previously, only a few Raman studies had been reported for oxomolybdoenzymes[17,18] and for reasonable models of these enzymes.[19-21] The paucity of Raman data for these molybdenum systems is due, in part, to the added

(1) (a) Oregon Graduate Institute of Science and Technology. (b) University of Arizona.
(2) (a) Mitchell, P. C. H. *Q. Rev., Chem. Soc.* **1966**, 103. (b) Mitchell, P. C. H. *Coord. Chem. Rev.* **1966**, *1*, 315. (c) Stiefel, E. I. *Prog. Inorg. Chem.* **1977**, *22*, 1.
(3) Young, C. G.; Enemark, J. H.; Collison, D.; Mabbs, F. E. *Inorg. Chem.* **1987**, *26*, 2925.
(4) Garner, C. D.; Bristow, S. In *Molybdenum Enzymes*; Spiro, T. G., Ed.; Wiley: New York, 1985; p 343.
(5) Wieghardt, K.; Hahn, M.; Weiss, J.; Swiridoff, W. *Z. Anorg. Allg. Chem.* **1982**, *492*, 164.
(6) (a) Wilson, G. L.; Kony, M.; Tiekink, E. R. T.; Pilbrow, J. R.; Spence, J. T.; Wedd, A. G. *J. Am. Chem. Soc.* **1988**, *110*, 6923. (b) Farchione, F.; Hansen, G. R.; Rodriguez, C. G.; Bailey, T. D.; Baghi, R. N.; Bond, A. M.; Pilbrow, J. R.; Wedd, A. G. *J. Am. Chem. Soc.* **1986**, *108*, 831.
(7) Johnson, J. L.; Rajagopalan, K. V. *Proc. Natl. Acad. Sci. U.S.A.* **1982**, *79*, 6856.
(8) (a) Hille, R.; Massey, V. In *Molybdenum Enzymes*; Spiro, T. G., Ed.; Wiley: New York, 1985; p 443. (b) Bray, R. C. *Q. Rev. Biophys.* **1988**, *21*, 5992.
(9) Cramer, S. P.; Wahl, R.; Rajagopalan, K. V. *J. Am. Chem. Soc.* **1981**, *103*, 7721.
(10) Bordas, J.; Bray, R. C.; Garner, C. D.; Gutteridge, S.; Hasnain, S. S. *Biochem. J.* **1980**, *191*, 499.
(11) Bray, R. C. *Adv. Enzymol. Relat. Areas Mol. Biol.* **1980**, *51*, 107.
(12) George, G. N.; Kipke, C. A.; Prince, R. C.; Sunde, R. A.; Enemark, J. H.; Cramer, S. P. *Biochemistry* **1989**, *28*, 5075.
(13) (a) Dowerah, D.; Spence, J. T.; Singh, R.; Wedd, A. G.; Wilson, G. L.; Farchione, F.; Enemark, J. H.; Kristofzski, J.; Bruck, M. *J. Am. Chem. Soc.* **1987**, *109*, 5655. (b) Hinshaw, C. J.; Spence, J. T. *Inorg. Chim. Acta* **1986**, *125*, L17.
(14) George, G. N.; Prince, R. C.; Kipke, C. A.; Sunde, R. A.; Enemark, J. H. *Biochem. J.* **1988**, *256*, 307.
(15) Minelli, M.; Enemark, J. H.; Wieghardt, K.; Hahn, M. *Inorg. Chem.* **1983**, *22*, 3952.
(16) For example: *Biological Applications of Raman Spectroscopy*; Resonance Raman Spectra of Heme and Metalloproteins, Vol. 3; Spiro, T. G., Ed.; Wiley: New York, 1988.
(17) Willis, L. J.; Loehr, T. M. *Biochemistry* **1985**, *24*, 2768.
(18) Garner, C. D.; Porter, T. G.; Wynn, C. H.; Alexander, R. S. Unpublished results cited in ref 4.
(19) Ueyama, N.; Nakata, M.; Araki, T.; Nakamura, A.; Yamashita, S.; Yamashita, T. *Inorg. Chem.* **1981**, *20*, 1934.
(20) (a) Willis, L. J.; Loehr, T. M.; Miller, K. F.; Bruce, A. E.; Stiefel, E. I. *Inorg. Chem.* **1986**, *25*, 4289. (b) Willis, L. J.; Loehr, T. M. *Spectrochim. Acta* **1987**, *43A*, 51.
(21) Lincoln, S. E.; Loehr, T. M. *Inorg. Chem.* **1990**, *29*, 1907.

0020-1669/91/1330-1839$02.50/0 © 1991 American Chemical Society